

GS: Generative Segmentation via Label Diffusion

Yuhao Chen¹, Shubin Chen¹, Liang Lin^{1 2 3}, Guangrun Wang^{1 2 3†}

¹Sun Yat-sen University, ² Guangdong Key Laboratory of Big Data Analysis and Processing, ³ X-Era AI Lab,

Abstract

Language-driven image segmentation is a fundamental task in vision-language understanding, requiring models to segment regions of an image corresponding to natural language expressions. Traditional methods approach this as a discriminative problem, assigning each pixel to foreground or background based on semantic alignment. Recently, diffusion models have been introduced to this domain, but existing approaches remain image-centric: they either (i) use image diffusion models as visual feature extractors, (ii) synthesize segmentation data via image generation to train discriminative models, or (iii) perform diffusion inversion to extract attention cues from pre-trained image diffusion models—thereby treating segmentation as an auxiliary process. In this paper, we propose **GS (Generative Segmentation)**, a novel framework that formulates segmentation itself as a generative task via *label diffusion*. Instead of generating images conditioned on label maps and text, GS reverses the generative process: it directly generates segmentation masks from noise, conditioned on both the input image and the accompanying language description. This paradigm makes label generation the primary modeling target, enabling end-to-end training with explicit control over spatial and semantic fidelity. To demonstrate the effectiveness of our approach, we evaluate GS on *Panoptic Narrative Grounding (PNG)*, a representative and challenging benchmark for multimodal segmentation that requires panoptic-level reasoning guided by narrative captions. Experimental results show that GS significantly outperforms existing discriminative and diffusion-based methods, setting a new state-of-the-art for language-driven segmentation.

1 Introduction

Image segmentation conditioned on natural language descriptions—often referred to as language-driven segmentation—has emerged as a critical capability for multimodal intelligence. Unlike traditional segmentation tasks that rely solely on visual cues, this task demands understanding and aligning both spatial and semantic information across modalities. Applications span referring expression segmentation, open-vocabulary mask generation, and panoptic narrative grounding.

Recent advances in diffusion models (Ho, Jain, and Abbeel 2020; Nichol and Dhariwal 2021) have led to re-

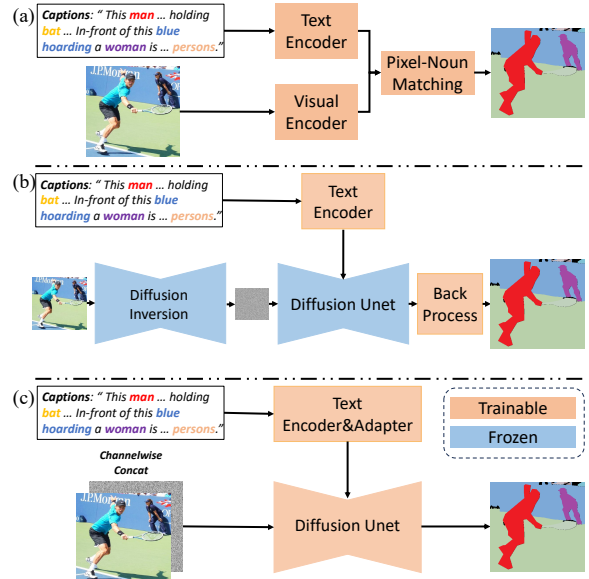


Figure 1: **Comparison of GS with prior segmentation paradigms.** (a) Discriminative models encode image and text into feature space and predict pixel-wise segmentation; this includes both traditional methods and diffusion-assisted approaches that rely on external discriminators. (b) Diffusion inversion methods extract attention maps from pre-trained image diffusion models for zero-shot grounding. (c) Our proposed GS directly performs label-space diffusion to generate segmentation masks from noise, conditioned on image and text, enabling end-to-end training without auxiliary components.

markable progress in generative modeling. Models like Stable Diffusion (Rombach et al. 2022) and ControlNet (Zhang, Rao, and Agrawala 2023) have demonstrated strong spatial reasoning and flexible conditioning capabilities, motivating their application to vision-language tasks. However, most diffusion-based segmentation methods remain fundamentally tied to the *image generation* process. Specifically, current approaches either: (1) extract features from frozen diffusion backbones for downstream discriminative models (Zhu et al. 2024), (2) generate synthetic segmentation data via diffusion to supervise segmentation models (Li et al. 2023c; Nguyen et al. 2023; Ma et al. 2023; Wu et al. 2023), or (3) perform inversion of image diffusion to extract intermediate attention maps for zero-shot grounding (Yang et al. 2024; Liu et al. 2024; Ni et al. 2023). These designsulti-

[†]Corresponding author.

mately treat segmentation as an auxiliary or post-hoc process, not the generative objective itself.

In this paper, we propose a new paradigm—**Generative Segmentation (GS)**—which reframes language-driven segmentation as a primary generative task. Rather than using diffusion to generate images, GS directly learns to generate segmentation masks from noise through a label-space diffusion process. Conditioned on both the input image and the language description, GS predicts a denoised segmentation map, effectively grounding linguistic concepts into precise pixel-wise masks. This task reversal—termed *label diffusion*—enables GS to perform structured mask generation directly, trained end-to-end without auxiliary stages or hand-crafted post-processing.

To evaluate our method, we adopt *Panoptic Narrative Grounding (PNG)* as a representative benchmark. PNG is one of the most comprehensive language-driven segmentation tasks to date, requiring models to segment both “things” and “stuff” in an image based on noun phrases extracted from free-form narrative captions.

A comparison between conventional panoptic narrative grounding methods and our label diffusion approach is illustrated in Fig. 1.

Our contributions are as follows:

1. We propose GS, a novel generative segmentation framework based on *label diffusion*, which directly generates segmentation masks conditioned on image and text inputs.
2. We introduce a dual-branch conditioning mechanism that injects spatial structure and semantic context into the generative process, enabling precise and faithful segmentation.
3. We demonstrate that GS achieves state-of-the-art performance on the Panoptic Narrative Grounding (PNG) benchmark, validating the strength and generality of our formulation.

2 Related Work

Diffusion Models for Segmentation. Diffusion models (Ho, Jain, and Abbeel 2020; Sohl-Dickstein et al. 2015) have become the foundation of high-fidelity image generation, achieving unprecedented performance in tasks such as text-to-image synthesis (Rombach et al. 2022) and structured conditioning (Zhang, Rao, and Agrawala 2023). Their capacity for spatial alignment and multimodal reasoning has inspired research into adapting them for vision-language segmentation. Existing efforts typically incorporate diffusion models in one of three ways: (1) as frozen feature extractors for downstream discriminative models (Zhu et al. 2024), (2) as generative engines for producing synthetic data to supervise segmentation models (Li et al. 2023c; Nguyen et al. 2023; Ma et al. 2023; Wu et al. 2023), or (3) through inversion techniques that extract attention maps for zero-shot localization (Yang et al. 2024; Liu et al. 2024; Ni et al. 2023). While effective, these designs use image generation as an intermediary and treat segmentation as a derived or auxiliary target.

In contrast, our work introduces **label diffusion**, which treats the segmentation mask itself as the object of generation. Rather than leveraging diffusion indirectly, our proposed GS model directly denoises segmentation masks from noise, conditioned on both visual and linguistic inputs. This formulation positions segmentation as a primary generative task, enabling explicit, structured alignment between image regions and language without reliance on handcrafted guidance or pretraining on external generation objectives. To our knowledge, GS is the first framework to perform language-driven segmentation via direct mask synthesis using conditional diffusion.

Generative Models for Visual Understanding. The idea of modeling data distributions to improve discriminative performance has a long history in computer vision. Early works (Hinton 2007; Ng and Jordan 2001) demonstrated that learning generative representations, could enhance downstream tasks like image classification by uncovering latent structure in the data. More recently, generative models have proven effective for learning representations applicable to both global and dense prediction tasks, including classification (Li et al. 2023b; Wang et al. 2022) and segmentation (Baranchuk et al. 2021). However, most of these approaches either train discriminative and generative objectives jointly, or fine-tune generative backbones for downstream tasks—treating generation as a pretext task rather than a means of direct prediction.

Diffusion models (Ho, Jain, and Abbeel 2020; Sohl-Dickstein et al. 2015) have emerged as particularly expressive generative frameworks, achieving strong results in image synthesis (Dhariwal and Nichol 2021; Rombach et al. 2022), while exhibiting powerful spatial reasoning and cross-modal alignment. Recent extensions such as Control-Net (Zhang, Rao, and Agrawala 2023) introduce controllable generation using structural priors like edges and depth, while pre-trained models such as Segment Anything (Kirillov et al. 2023) leverage foundation vision models for open-vocabulary region parsing. Nevertheless, the majority of prior work leverages diffusion models indirectly—either as feature extractors, data generators, or through inversion pipelines—and does not directly use the generative process itself to perform task-specific predictions like segmentation or classification (Li et al. 2023a).

In this work, we take a different route. Instead of treating generation as auxiliary, we model segmentation as a primary generative objective via a conditional label-space diffusion process. Our method, GS, demonstrates that diffusion models can directly synthesize structured outputs such as segmentation masks from noise, conditioned on image and text. This contributes to a relatively underexplored direction: using generative models not just for representation learning, but for direct, interpretable predictions.

Panoptic Narrative Grounding. Panoptic Narrative Grounding (PNG) (González et al. 2021) is a challenging vision-language task that generalizes referring segmentation to panoptic-level coverage. It requires associating free-form narrative captions with precise segmentation masks of both “thing” objects and “stuff” regions. Compared to

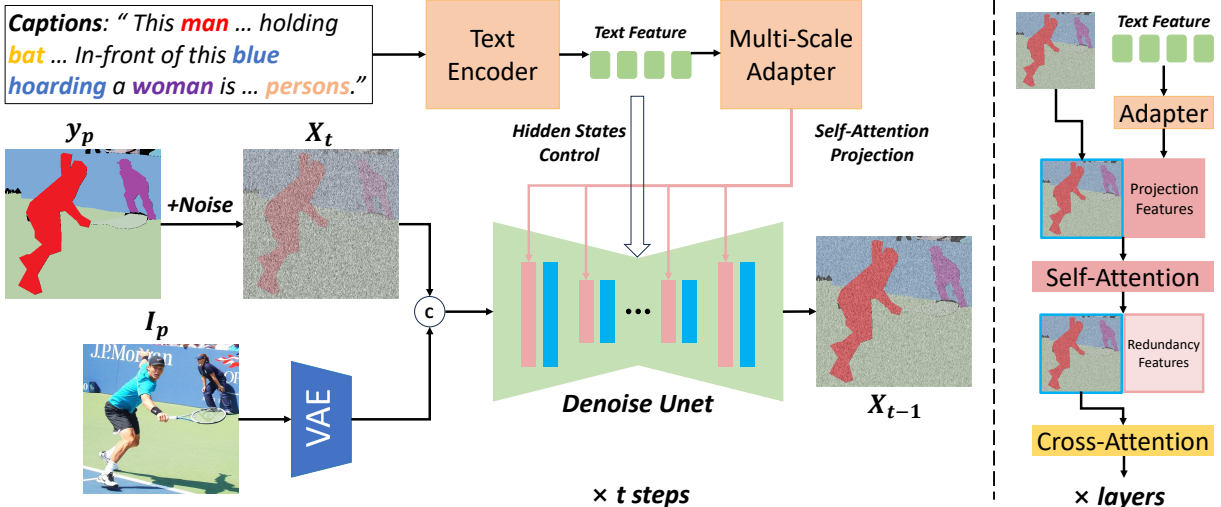


Figure 2: **Overview of GS.** Our Generative Segmentation (GS) framework synthesizes segmentation masks via a conditional label-space diffusion process. During training, ground-truth masks are noised in the latent space and denoised by a U-Net conditioned on both the input image and the associated text. The image is encoded by a VAE and concatenated channel-wise to the noisy label. Text guidance is incorporated through global CLIP embeddings and multi-scale adapter features, which are injected into the U-Net via token-level attention as well as cross-attention. We apply classifier-free guidance by randomly dropping text conditions during training and combining conditional and unconditional predictions at test time. GS directly generates high-quality segmentation masks without relying on intermediate RGB synthesis.

traditional referring expression segmentation, PNG incorporates multiple noun phrases per image and demands modeling of complex linguistic structures including coreference, spatial relations, and attribute composition. Prior approaches primarily adopt discriminative pipelines that combine cross-modal encoders with per-phrase segmentation heads (González et al. 2021; Li et al. 2024). Recent variants enhance grounding quality using vision-language pretraining (e.g., CLIP) or use image generation diffusion models for feature encoding. However, these designs do not model mask synthesis as a generative process.

We adopt PNG as a representative benchmark to evaluate our proposed GS framework due to its comprehensive multimodal nature. The complexity of PNG highlights GS’s capability in simultaneously resolving linguistic reference and spatial mask generation through a unified, end-to-end generative process.

3 Methods

We introduce **GS (Generative Segmentation)**, a framework that directly generates segmentation masks via a conditional label-space diffusion process. Unlike previous approaches that rely on image synthesis pipelines, GS treats segmentation as a primary generative task. At the core of GS is a denoising model that generates pixel-wise masks from noise, guided jointly by the input image and a textual description. Fig. 2 provides an overview of our framework.

We evaluate GS on the Panoptic Narrative Grounding (PNG) task, a comprehensive benchmark involving language-conditioned segmentation. However, GS is general and applicable to a wide range of language-driven segmentation settings.

3.1 Notation

We summarize the key notations used throughout this paper in Table 1. These notations define the image, language, and diffusion components used in our generative segmentation framework.

Symbol	Description
$\mathcal{I} \in \mathbb{R}^{H \times W \times 3}$	Input image
\mathcal{T}	Natural language caption associated with \mathcal{I}
T_i	The i -th noun phrase extracted from \mathcal{T}
$y_i \in \mathbb{R}^{H \times W}$	Ground-truth segmentation mask for T_i
$\tilde{y}_i \in \mathbb{R}^{H \times W}$	Predicted segmentation mask for T_i
$\varepsilon(\cdot)$	Variational autoencoder used for latent encoding
x_0	Clean label (segmentation mask) in latent space
x_t	Noisy label at diffusion timestep t
$\epsilon \sim \mathcal{N}(0, I)$	Standard Gaussian noise
$\bar{\alpha}_t$	Predefined noise schedule at timestep t
e^t_i	Text embedding of noun phrase T_i from CLIP encoder
e^p_{il}	Layer-wise projected feature from adapter at U-Net layer l
$\Phi(\cdot)$	U-Net denoising network
X_l	Input feature at layer l of U-Net

Table 1: **Summary of notations used in GS.**

3.2 Preliminaries

Language-Driven Segmentation. Language-driven segmentation refers to the task of generating pixel-wise segmentation masks $y_i \in \mathbb{R}^{H \times W}$ that correspond to natural language expressions T_i , where i denotes the index of the i -th noun phrase in a given textual description. Given an input image $\mathcal{I} \in \mathbb{R}^{H \times W \times 3}$ and an associated caption \mathcal{T} , the objective is to identify and localize all referential noun phrases T_i within \mathcal{T} , and to produce accurate segmentation masks y_i aligned with each phrase. In this work, we adopt the Panoptic Narrative Grounding (PNG) benchmark (González et al.

2021) as the primary evaluation setting, as it provides dense linguistic supervision and panoptic-level mask annotations.

Diffusion Modeling. Diffusion models (Ho, Jain, and Abbeel 2020) are a class of generative models that learn to approximate complex data distributions through a denoising process. They consist of two stages: a forward (noising) process that gradually adds Gaussian noise to the input data over a series of timesteps, and a reverse (denoising) process learned by a neural network. Given a clean data sample x_0 , the forward process generates a noisy version x_t at timestep t as:

$$x_t = \sqrt{\bar{\alpha}_t}x_0 + \sqrt{1 - \bar{\alpha}_t}\epsilon, \quad \epsilon \sim \mathcal{N}(0, I), \quad (1)$$

where $\bar{\alpha}_t$ is a predefined noise schedule. The model is trained to predict the noise ϵ added at each timestep, thereby learning to reverse the noising process and sample clean data from pure noise.

3.3 Label Diffusion for Generative Segmentation

Unlike traditional diffusion models that operate over natural images, our formulation performs denoising in the *label space*, where the clean signal $x_0 \in \mathbb{R}^{\frac{H}{8} \times \frac{W}{8} \times 1}$ represents the ground-truth segmentation mask in latent form. At each diffusion timestep t , we aim to recover x_0 from its noisy counterpart x_t , conditioned on both the input image \mathcal{I} and the corresponding noun phrase T_i .

To this end, we model the conditional denoising process as:

$$\tilde{\epsilon}_t = \Phi(\text{concat}_{\text{channel}}(x_t, \varepsilon(\mathcal{I})), t, e_i^t, e_{il}^p), \quad (2)$$

where:

- x_t is the noisy label map at timestep t ,
- $\varepsilon(\mathcal{I}) \in \mathbb{R}^{\frac{H}{8} \times \frac{W}{8} \times 4}$ is the VAE-encoded image latent,
- $\text{concat}(\cdot, \cdot)$ denotes channel-wise concatenation,
- $e_i^t = \text{CLIP}(T_i)$ is the global text embedding of the noun phrase T_i ,
- $e_{il}^p = \text{Adapter}_l(e_i^t)$ is the projected text feature injected into the U-Net at layer l ,
- Φ is the denoising U-Net.

In this formulation, the image serves as a spatial condition via channel-wise concatenation to the noisy label, while the text provides semantic conditioning through cross-attention and multi-scale injection mechanisms. These two fusion pathways allow GS to align both spatial and linguistic cues when generating segmentation masks. Details of these fusion mechanisms are discussed in the next section.

3.4 Multi-Scale Feature Injection

As we mention, the text provides semantic conditioning through cross-attention and multi-scale injection mechanisms. Since the cross attention is traditional, we will only describe multi-scale injection here.

Latent Space Embedding. We adopt SDXL (Rombach et al. 2022) as the backbone diffusion model, operating in the latent space defined by a variational autoencoder ε . The image \mathcal{I} is encoded to $\varepsilon(\mathcal{I}) \in \mathbb{R}^{\frac{H}{8} \times \frac{W}{8} \times 4}$, which is concatenated with the noisy label map at each diffusion step.

Token-Level Adapter Injection. To enable fine-grained alignment between vision and language, we follow prior work (Choi et al. 2024) and inject adapter features into the self-attention layers of the U-Net. Specifically, for each U-Net layer l , the input feature map $X_l \in \mathbb{R}^{N \times C}$ (flattened spatial tokens) is concatenated with the projected text features $e_{il}^p \in \mathbb{R}^{M \times C}$ along the token dimension, yielding the joint token sequence:

$$A = \text{concat}_{\text{token}}(X_l, e_{il}^p) \in \mathbb{R}^{(N+M) \times C}. \quad (3)$$

This joint sequence is then processed by the self-attention mechanism:

$$Z = \text{Attention}(AW^Q, AW^K, AW^V)W^O \in \mathbb{R}^{(N+M) \times C}, \quad (4)$$

where W^Q, W^K, W^V, W^O are the learned projection matrices. Finally, we discard the output tokens corresponding to the text embeddings and retain only the updated image features:

$$Y_l = Z_{1:N,:} \in \mathbb{R}^{N \times C}, \quad (5)$$

which are forwarded to the next U-Net layer. This design allows image tokens to attend to the injected language signals while preventing the injected tokens from contributing residual noise to downstream layers.

3.5 Training and Inference with Classifier-Free Guidance

Training via Conditional Dropout. To enable classifier-free guidance (Ho and Salimans 2022), we apply stochastic conditioning dropout during training. Specifically, with a fixed probability p_{drop} , we replace the text embedding e_i^t and the projected adapter features e_{il}^p with learned null embeddings (“none” tokens), effectively simulating unconditioned denoising:

$$\tilde{\epsilon}_t = \Phi(\text{concat}_{\text{channel}}(x_t, \varepsilon(\mathcal{I})), t, \tilde{e}_i^t, \tilde{e}_{il}^p), \quad (6)$$

where $\tilde{e}_i^t \leftarrow \text{Drop}(e_i^t)$, $\tilde{e}_{il}^p \leftarrow \text{Drop}(e_{il}^p)$, and Drop denotes random replacement with null tokens with probability p_{drop} . The training objective minimizes the denoising prediction loss:

$$\mathcal{L} = \mathbb{E}_{x_t, \epsilon} [\|\epsilon - \tilde{\epsilon}_t\|^2]. \quad (7)$$

Inference via Classifier-Free Guidance. At inference time, we leverage both conditional and unconditional denoising predictions to improve semantic alignment. Specifically, we perform two forward passes of the U-Net at each timestep t :

$$\epsilon_{\text{cond}} = \Phi(x_t, t, e_i^t, e_{il}^p), \quad (8)$$

$$\epsilon_{\text{uncond}} = \Phi(x_t, t, \text{None}, \text{None}), \quad (9)$$

and apply the classifier-free guidance formula to interpolate:

$$\epsilon_{\text{guided}} = \epsilon_{\text{uncond}} + w \cdot (\epsilon_{\text{cond}} - \epsilon_{\text{uncond}}), \quad (10)$$

where $w \geq 1$ is the guidance scale. The denoising step then uses ϵ_{guided} to update the latent:

$$x_{t-1} = \text{DenoiseStep}(x_t, \epsilon_{\text{guided}}, t), \quad (11)$$

where DenoiseStep follows the standard DDPM update rule. After T steps, we obtain the final prediction \tilde{y}_i by decoding x_0 and resizing to the target resolution.

Method	Venue	Diffusion	P.S. Pretrain	Average Recall(\uparrow)				
				overall	things	stuff	singulars	plurals
DiffSeg (Tian et al. 2024)	CVPR24	✓	✗	24.1	17.7	33.0	24.8	18.0
DiffPNG (Yang et al. 2024)	ECCV24	✓	✗	38.5	36.0	42.0	39.2	32.1
EPNG (Wang et al. 2023b)	AAAI23	✗	✗	49.7	45.6	55.5	50.2	45.1
MCN (Luo et al. 2020)	CVPR20	✗	✓	54.2	48.6	61.4	56.6	38.8
PNG (González et al. 2021)	ICCV21	✗	✓	55.4	56.2	54.3	56.2	48.8
PPMN (Ding et al. 2022)	ACMMM22	✗	✗	56.7	53.4	61.1	57.4	49.8
EPNG (Wang et al. 2023b)	AAAI23	✗	✓	58.0	54.8	62.4	58.6	52.1
PPMN (Ding et al. 2022)	ACMMM22	✗	✓	59.4	57.2	62.5	60.0	54.0
ODISE (Xu et al. 2023)	CVPR23	✓	✗	61.0	57.0	66.6	61.7	54.8
NICE (Wang et al. 2023a)	arXiv	✗	✓	62.3	60.2	65.3	63.1	55.2
DRMN (Lin et al. 2023)	ICDMI23	✗	✓	62.9	60.3	66.4	63.6	56.7
ODISE (Xu et al. 2023)	CVPR23	✓	✓	63.1	59.6	68.0	64.0	55.1
PiGLET (González et al. 2023)	TPAMI23	✗	✓	65.9	64.0	68.6	67.2	54.5
PPO-TD (Hui et al. 2023)	IJCAI23	✗	✓	66.1	63.3	69.8	66.9	58.6
EIPA+MLMA (Li et al. 2024)	ACMMM24	✗	✓	67.1	64.3	71.0	67.9	60.0
GS(Ours)	-	✓	✗	69.7	65.6	76.5	71.3	63.7

Table 2: **Comparison with previous state-of-the-art methods on the PNG benchmark.** Our comparison on Average Recall metric includes 5 items: the overall average recall and four subcategories things and stuff categories, and singulars and plurals noun phrases. “P.S. Pretrain” denotes visual panoptic segmentation pretraining on COCO. The highest performances are reported among different model architectures.

4 experiment

4.1 Datasets and Evaluation Protocol

Datasets Following prior works, we train and evaluate our method on the **Panoptic Narrative Grounding** dataset. The PNG dataset establishes a large-scale multimodal benchmark by combining the narrative captions annotated in the **Localized Narratives** dataset with the panoptic segmentation annotated in the COCO dataset. The visual part of the dataset is based on the famous **COCO** dataset, with 133,103 images for training and 8533 images for validation. The PNG benchmark contains 726,445 noun phrases aligned with 741,697 segmentation masks, forming caption-image annotation pairs. Each caption averages 11.3 noun phrases, of which 5.1 necessitate grounding via segmentation masks. It should be noted that the noun phrases in the dataset are disaggregated into things and stuff categories, and singulars and plurals noun phrases.

Metrics The Average Recall (AR) metric in the PNG benchmark quantifies open-vocabulary segmentation recall robustness through multi-threshold IoU analysis. Computed as the mean recall across 10,000 distinct Intersection-over-Union thresholds ($\tau \in \{0.0001, 0.0002, \dots, 0.9999\}$), AR evaluates a model’s ability to ground all noun phrases in narrative captions to precise spatial extents. For each noun phrase T_{ip} and its ground-truth mask y_p , a predicted mask \tilde{y}_p is considered correctly recalled at threshold τ iff $IoU(\tilde{y}_p, y_p) \geq \tau$. The final AR aggregates recall rates across all phrases and images:

$$AR = \frac{1}{10,000} \sum_{\tau} \frac{\sum_p \text{CorrectRecallPhrases}(\tau)}{\sum_p \text{TotalPhrases}(\tau)}, \quad (12)$$

where p presents the index of the picture.

Corresponding to the two paired attributes of noun phrases, the AR metric also comprises four sub-categories: AR_{things} , AR_{stuff} , $AR_{singulars}$ and $AR_{plurals}$. Each reflecting method performance on their respective categories.

4.2 Implementation Details

Our framework is implemented with PyTorch. We use SDXL inpainting model for the core diffusion pipeline and 2 different linear layers for the multi-scale adapter module. For stable diffusion, the total step is 1000, the DDIM diffusion step is 50 and the guidance scale is set to 7.5. Our model is trained using Adam optimizer with batch size of 128 and learning rate of 1e-7 for 10 epochs.

4.3 Results and Analysis

To evaluate our model, we conducted visual quality testing and quantitative metric testing on the PNG image dataset, achieving outstanding performance. Additionally, we tested it on real-world images, demonstrating the method’s excellent generalization ability.

Qualitative Results. In Fig. 3. we visualized the outputs of our method on representative samples from the PNG dataset. Benefiting from the inherent smoothness of the diffusion model’s generative process, our segmentation masks exhibit softer contours at the boundaries compared to the ground truth, thereby more precisely adhering to the target objects. For example, in (a), the image shows a man next to a traffic light and the ground truth failed to fully cover the target object, leaving an unlabeled perimeter around its edges, whereas our approach successfully segmented the entire traffic light. And in Fig. 4, the image depicts a dog lying on a sofa holding a shoe in its embrace. While the ground truth incorrectly segmented the upper portion of the shoe as

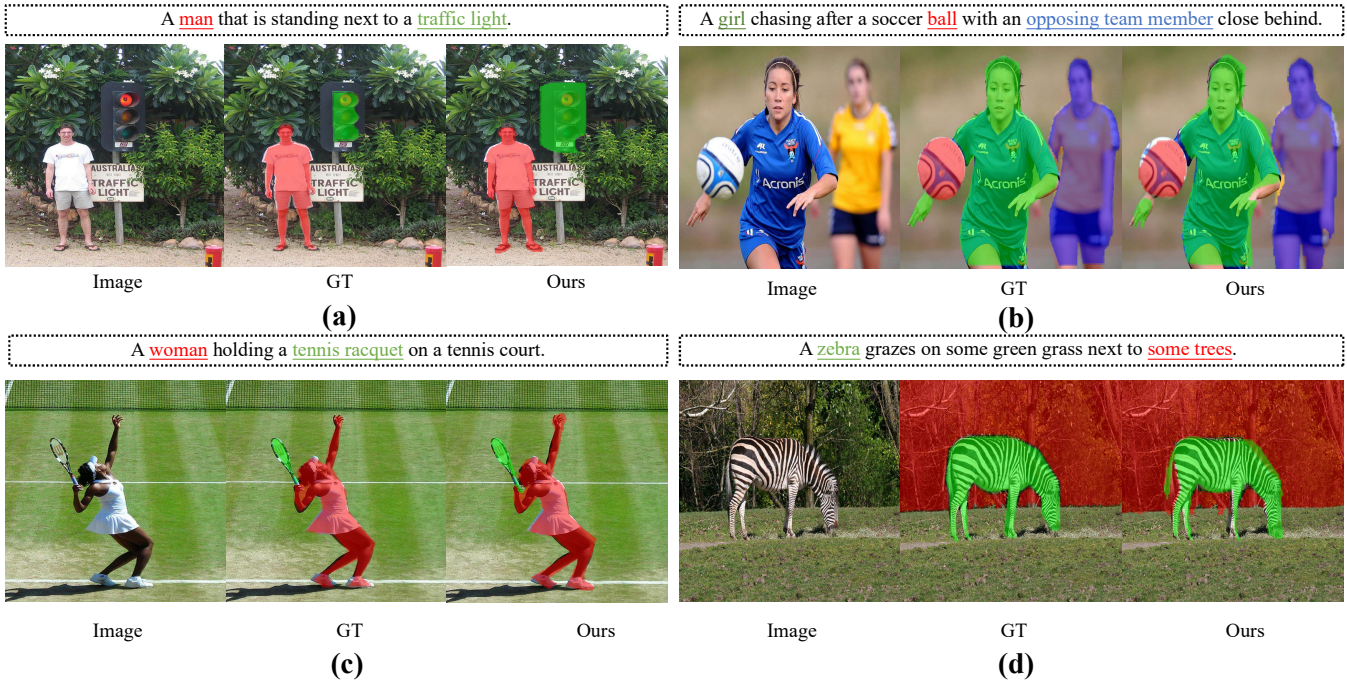


Figure 3: **Visualization of GS on representational samples on the PNG dataset.** All visualized images belong to the test set.

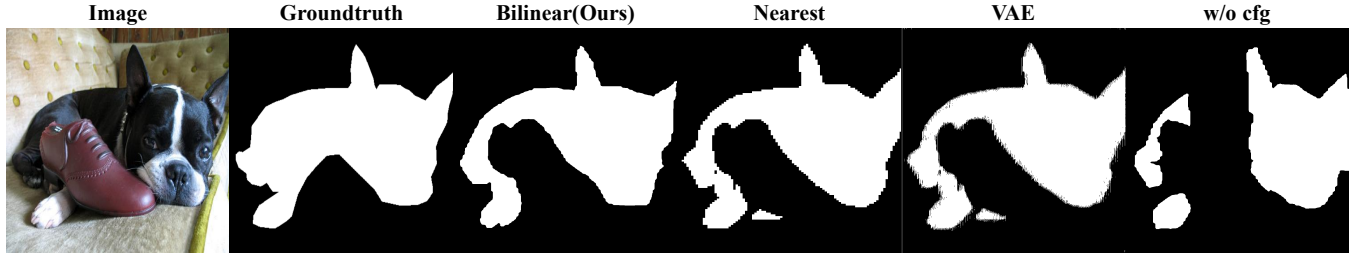


Figure 4: **Comparison with different post-processing techniques on final mask.** Notably, our bilinear interpolation method with classifier-free guidance (cfg) achieves superior results compared to gt. Furthermore, naive linear interpolation causes serrated edges, VAE decoding introduces undesired artifacts, and interpolation without cfg results in weaker conditional control.

part of the dog, our model remained unaffected by this ambiguity and robustly segmented the occluded shoe.

We then demonstrate the impact of different post-processing techniques on final mask quality in Fig. 4: First, using the VAE decoder to generate masks is a natural approach. However, as observed in our results, the VAE is susceptible to residual noise in the latent space, producing masks with artifacts. Second, nearest-neighbor interpolation results in more pronounced jagged edges compared to bilinear interpolation, degrading visual quality. Finally, inference without Classifier-Free Guidance (CFG) diminishes textual conditioning during generation, leading to detrimental visual outcomes.

Quantitative Results. As shown in table 2, we presents a comparative analysis of various methods on the PNG benchmark using the Average Recall metric.

Among the evaluated methods, our proposed GS (Ours) achieves the state-of-the-art performance in terms of overall Average Recall, with a value of 69.7. When examining the

sub - categories, it also outperforms other methods in “stuff” (76.5), “singulars” (71.3), and “plurals” (63.7) Average Recall. The “things” metric indicates our model underperforms counterparts on individual objects. Based on ablation studies across image sizes, we hypothesize that the constrained latent space dimensions in the VAE encoder impair this capability. Adopting larger image resolutions is expected to substantially enhance performance in this aspect.

As the first end-to-end generative approach, our GS achieves state-of-the-art performance among both diffusion-based and pixel-noun matching methods. Zero-shot Stable Diffusion frameworks like DiffSeg(Tian et al. 2024) and DiffPNG(Yang et al. 2024) suffer from their non-trainable nature, yielding suboptimal results. Feature-extraction fine-tuning methods such as ODISE(Xu et al. 2023) and EIPA+MLMA(Li et al. 2024) fall short of our approach.

Notably, our method without pretraining outperforms other pretrained counterparts, even though the table shows that pretraining on COCO panoptic segmentation task sig-

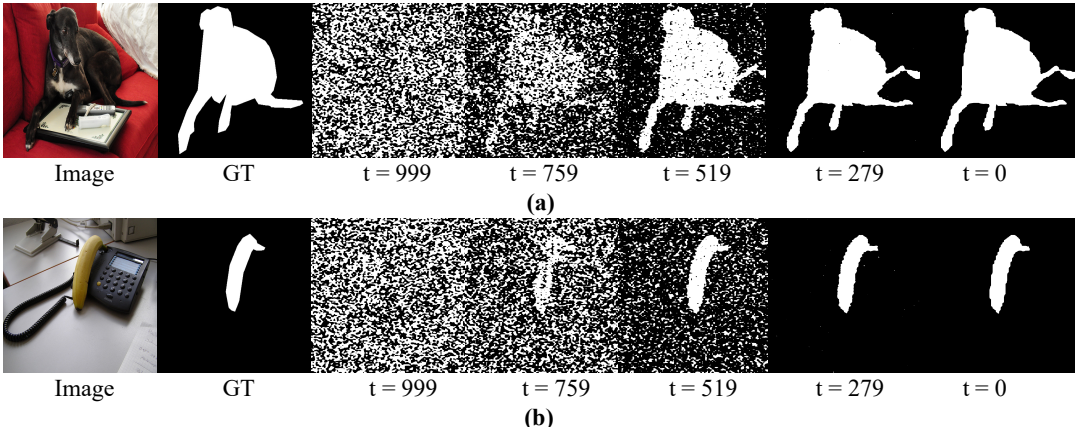


Figure 5: **Time-series Visualization of Images and Ground Truth for GS Samples on the PNG Dataset.** All visualized images belong to the test set. The figures are divided into two parts (a) and (b). Each part contains “Image” and “GT” columns, with the time steps $t=0$, $t=279$, $t=519$, $t=759$, and $t=999$ displayed to show the evolutionary process of the samples at different moments.

Size	Average Recall(\uparrow)				
	overall	things	stuff	singulars	plurals
(1024, 1024)	71.0	66.3	78.0	70.9	71.5
(768, 768)	64.6	62.1	68.3	64.3	65.6
(512, 512)	32.7	24.4	45.6	33.1	31.3

Table 3: **Ablations on various image size.**

Steps	Average Recall(\uparrow)				
	overall	things	stuff	singulars	plurals
50	71.0	66.3	78.0	70.9	71.5
30	69.3	64.8	76.3	69.0	70.8
20	68.7	63.9	76.2	68.5	69.9

Table 4: **Ablations on DDIM steps**

nificantly enhances model performance. This demonstrates the pioneering nature and effectiveness of our GS method in adapting diffusion models to the panoptic narrative grounding task.

4.4 Ablation Study

In this subsection, we conducted comprehensive ablation studies to investigate the impact of different design choices on segmentation quality. The ablation study was conducted on a subset of the test set, comprising approximately 7% of its total size. The experiments focused on three key parameter factors: generated image size, DDIM steps, and guidance scale.

Image Size. This subsection investigates the critical impact of the generated image size on the performance and output quality of GS. In table 3, we can see the overall accuracy decreases proportionally with the reduction in generated image size. We attribute this performance degradation to insufficient spatial information in undersized images. Due to the limited receptive field, the model produces less precise masks, which particularly impacts the ‘things’ and ‘singulars’ subcategories that require higher segmentation precision.

Guidance Scale	Average Recall(\uparrow)				
	overall	things	stuff	singulars	plurals
7.5	71.0	66.3	78.0	70.9	71.5
8.0	70.5	66.9	76.3	70.4	71.3
7.0	70.7	67.0	76.6	70.7	71.1

Table 5: **Ablations on Guidance Scale.**

DDIM Steps. Here, we focus on ablating the number of sampling steps in the denoising diffusion implicit model (DDIM) process. In table 4, the increasing the number of sampling steps allows for finer-grained capture of the data distribution, potentially enhancing both the accuracy and detail of the generated results. By incrementally reducing the step count from a baseline high value, we observe a slight performance degradation in the model, which aligns with theoretical expectations of DDIM.

Guidance Scale. The third ablation study examines the influence of the classifier-free guidance scale, a key hyperparameter controlling the trade-off between sample diversity and fidelity to the conditioning signal (e.g., text prompt). We conducted exploratory investigations in the neighborhood of the empirically determined guidance scale parameter, which confirmed the optimality of the original empirical value.

4.5 Applicable Efficiency.

Our accurate segmentation approach consists of a lightweight adapter and a performance-optimized SDXL pipeline. On an A100 GPU, a single inference pass with a batch size of 16 takes only 50 seconds, averaging just 3 seconds per image generated.

5 Conclusion

We introduced **GS**, a novel framework that formulates language-driven segmentation as a generative task via *label diffusion*. In contrast to existing image-centric approaches that treat segmentation as a downstream or auxiliary objective, GS directly generates segmentation masks from noise

conditioned on both visual and linguistic inputs. This reorientation makes the label space the central modeling target, enabling more faithful spatial and semantic grounding.

To support this paradigm, we designed a dual conditioning mechanism that integrates image structure and textual semantics into the generative process through latent fusion and multi-scale adapter injection. Experimental results on the Panoptic Narrative Grounding benchmark demonstrate that GS achieves new state-of-the-art performance, highlighting the effectiveness and generality of treating segmentation as generative modeling. We believe GS opens a promising direction for unifying generative modeling and structured prediction in multimodal tasks.

References

Baranchuk, D.; Rubachev, I.; Voynov, A.; Khrulkov, V.; and Babenko, A. 2021. Label-efficient semantic segmentation with diffusion models. *arXiv preprint arXiv:2112.03126*.

Choi, Y.; Kwak, S.; Lee, K.; Choi, H.; and Shin, J. 2024. Improving diffusion models for authentic virtual try-on in the wild. In *European Conference on Computer Vision*, 206–235. Springer.

Dhariwal, P.; and Nichol, A. 2021. Diffusion models beat gans on image synthesis. *Advances in neural information processing systems*, 34: 8780–8794.

Ding, Z.; Ding, Z.-h.; Hui, T.; Huang, J.; Wei, X.; Wei, X.; and Liu, S. 2022. Ppmn: Pixel-phrase matching network for one-stage panoptic narrative grounding. In *Proceedings of the 30th ACM International Conference on Multimedia*, 5537–5546.

González, C.; Ayobi, N.; Hernández, I.; Hernández, J.; Pont-Tuset, J.; and Arbeláez, P. 2021. Panoptic narrative grounding. In *Proceedings of the IEEE/CVF International Conference on Computer Vision*, 1364–1373.

González, C.; Ayobi, N.; Hernández, I.; Pont-Tuset, J.; and Arbeláez, P. 2023. Piglet: Pixel-level grounding of language expressions with transformers. *IEEE Transactions on Pattern Analysis and Machine Intelligence*, 45(10): 12206–12221.

Hinton, G. E. 2007. To recognize shapes, first learn to generate images. *Progress in brain research*, 165: 535–547.

Ho, J.; Jain, A.; and Abbeel, P. 2020. Denoising diffusion probabilistic models. *Advances in neural information processing systems*, 33: 6840–6851.

Ho, J.; and Salimans, T. 2022. Classifier-free diffusion guidance. *arXiv preprint arXiv:2207.12598*.

Hui, T.; Ding, Z.; Huang, J.; Wei, X.; Wei, X.; Dai, J.; Han, J.; and Liu, S. 2023. Enriching phrases with coupled pixel and object contexts for panoptic narrative grounding. *arXiv preprint arXiv:2311.01091*.

Kirillov, A.; Mintun, E.; Ravi, N.; Mao, H.; Rolland, C.; Gustafson, L.; Xiao, T.; Whitehead, S.; Berg, A. C.; Lo, W.-Y.; et al. 2023. Segment anything. In *Proceedings of the IEEE/CVF international conference on computer vision*, 4015–4026.

Li, A. C.; Prabhudesai, M.; Duggal, S.; Brown, E.; and Pathak, D. 2023a. Your diffusion model is secretly a zero-shot classifier. In *Proceedings of the IEEE/CVF International Conference on Computer Vision*, 2206–2217.

Li, H.; Hui, T.; Ding, Z.; Zhang, J.; Ma, B.; Wei, X.; Han, J.; and Liu, S. 2024. Dynamic prompting of frozen text-to-image diffusion models for panoptic narrative grounding. In *Proceedings of the 32nd ACM International Conference on Multimedia*, 9485–9494.

Li, T.; Chang, H.; Mishra, S.; Zhang, H.; Katabi, D.; and Krishnan, D. 2023b. Mage: Masked generative encoder to unify representation learning and image synthesis. In *Proceedings of the IEEE/CVF Conference on Computer Vision and Pattern Recognition*, 2142–2152.

Li, Z.; Zhou, Q.; Zhang, X.; Zhang, Y.; Wang, Y.; and Xie, W. 2023c. Open-vocabulary object segmentation with diffusion models. In *Proceedings of the IEEE/CVF International Conference on Computer Vision*, 7667–7676.

Lin, Y.; Jin, X.-B.; Wang, Q.; and Huang, K. 2023. Context does matter: end-to-end panoptic narrative grounding with deformable attention refined matching network. In *2023 IEEE International Conference on Data Mining (ICDM)*, 1163–1168. IEEE.

Liu, X.; Huang, S.; Kang, Y.; Chen, H.; and Wang, D. 2024. Vgdiffzero: Text-to-image diffusion models can be zero-shot visual grounders. In *ICASSP 2024-2024 IEEE International Conference on Acoustics, Speech and Signal Processing (ICASSP)*, 2765–2769. IEEE.

Luo, G.; Zhou, Y.; Sun, X.; Cao, L.; Wu, C.; Deng, C.; and Ji, R. 2020. Multi-task collaborative network for joint referring expression comprehension and segmentation. In *Proceedings of the IEEE/CVF Conference on computer vision and pattern recognition*, 10034–10043.

Ma, C.; Yang, Y.; Ju, C.; Zhang, F.; Liu, J.; Wang, Y.; Zhang, Y.; and Wang, Y. 2023. Diffusionseg: Adapting diffusion towards unsupervised object discovery. *arXiv preprint arXiv:2303.09813*.

Ng, A.; and Jordan, M. 2001. On discriminative vs. generative classifiers: A comparison of logistic regression and naive bayes. *Advances in neural information processing systems*, 14.

Nguyen, Q.; Vu, T.; Tran, A.; and Nguyen, K. 2023. Dataset diffusion: Diffusion-based synthetic data generation for pixel-level semantic segmentation. *Advances in Neural Information Processing Systems*, 36: 76872–76892.

Ni, M.; Zhang, Y.; Feng, K.; Li, X.; Guo, Y.; and Zuo, W. 2023. Ref-diff: Zero-shot referring image segmentation with generative models. *arXiv preprint arXiv:2308.16777*.

Nichol, A. Q.; and Dhariwal, P. 2021. Improved denoising diffusion probabilistic models. In *International conference on machine learning*, 8162–8171. PMLR.

Rombach, R.; Blattmann, A.; Lorenz, D.; Esser, P.; and Ommer, B. 2022. High-resolution image synthesis with latent diffusion models. In *Proceedings of the IEEE/CVF conference on computer vision and pattern recognition*, 10684–10695.

Sohl-Dickstein, J.; Weiss, E.; Maheswaranathan, N.; and Ganguli, S. 2015. Deep unsupervised learning using nonequilibrium thermodynamics. In *International conference on machine learning*, 2256–2265. pmlr.

Tian, J.; Aggarwal, L.; Colaco, A.; Kira, Z.; and Gonzalez-Franco, M. 2024. Diffuse attend and segment: Unsupervised zero-shot segmentation using stable diffusion. In *Proceedings of the IEEE/CVF Conference on Computer Vision and Pattern Recognition*, 3554–3563.

Wang, G.; Tang, Y.; Lin, L.; and Torr, P. H. 2022. Semantic-aware auto-encoders for self-supervised representation learning. In *Proceedings of the IEEE/CVF Conference on Computer Vision and Pattern Recognition*, 9664–9675.

Wang, H.; Ji, J.; Guo, T.; Yang, Y.; Zhou, Y.; Sun, X.; and Ji, R. 2023a. Nice: improving panoptic narrative detection and segmentation with cascading collaborative learning. *arXiv preprint arXiv:2310.10975*.

Wang, H.; Ji, J.; Zhou, Y.; Wu, Y.; and Sun, X. 2023b. Towards real-time panoptic narrative grounding by an end-to-end grounding network. In *Proceedings of the AAAI Conference on Artificial Intelligence*, volume 37, 2528–2536.

Wu, W.; Zhao, Y.; Shou, M. Z.; Zhou, H.; and Shen, C. 2023. Diffumask: Synthesizing images with pixel-level annotations for semantic segmentation using diffusion models. In *Proceedings of the IEEE/CVF International Conference on Computer Vision*, 1206–1217.

Xu, J.; Liu, S.; Vahdat, A.; Byeon, W.; Wang, X.; and De Mello, S. 2023. Open-vocabulary panoptic segmentation with text-to-image diffusion models. In *Proceedings of the IEEE/CVF conference on computer vision and pattern recognition*, 2955–2966.

Yang, D.; Dong, R.; Ji, J.; Ma, Y.; Wang, H.; Sun, X.; and Ji, R. 2024. Exploring phrase-level grounding with text-to-image diffusion model. In *European Conference on Computer Vision*, 161–180. Springer.

Zhang, L.; Rao, A.; and Agrawala, M. 2023. Adding conditional control to text-to-image diffusion models. In *Proceedings of the IEEE/CVF international conference on computer vision*, 3836–3847.

Zhu, Z.; Feng, X.; Chen, D.; Yuan, J.; Qiao, C.; and Hua, G. 2024. Exploring pre-trained text-to-video diffusion models for referring video object segmentation. In *European Conference on Computer Vision*, 452–469. Springer.

A Supplementary Content

This is the supplementary material of paper **GS: Generative Segmentation via Label Diffusion**. We have included additional favorable visualization samples from the test set, along with problematic cases for reviewers' analysis. The source code and deployment instructions are also provided.

B Correct samples

In Fig. 6, we provide more samples that our model generates. In the **First Line** example, the two target prompts “person” and “umbrella” exhibit similar coloration and are spatially adjacent. Nevertheless, our model successfully delineates both targets with high precision through robust semantic alignment, effectively resisting visual interference. In the **Fourth Line** example, one target prompt “person” is neither centrally positioned nor constitutes a complete human figure; the other target “mobile phone” occupies minimal image area. Our model successfully segments both targets with high fidelity, validating its generalization capability for peripheral and partial objects, along with precise segmentation of small-scale objects.

C Failed samples

In Fig. 7, we provide some samples that our model failed to predict correct mask. In the **UP** example, for the segmentation target “hand”, the ground truth captures the entire girl, whereas our method erroneously segments only the lower body of the child. In the **DOWN** example, for the segmentation target “bench”, the ground truth correctly delineates the entire bench, whereas our method catastrophically classifies almost the entire scene as the bench.

Caption

Image

GT

Ours

In this image there is a **person** standing and holding **umbrella** inside a house where there are frames, light attached to wall and doors.



In the bottom of the image there is a ground with **grass** on it. In the middle of the image there is a **bench** ...



In this image I can see an **aircraft** and also I can see smoke over here.



In this image we can see a laptop, **mobile phone** and some things are kept on the table. In the background we can see a chair and a **person** standing near the table.



There is a **person** in blue color coat, wearing black color bag, ..., which is on the **snow** hill. In the background, there are trees, mountains and sky.



In this picture **deity** **players** standing on the ground. On the left there is a person who is wearing a **white dress** and holding a ball.



Figure 6: Visualization of Images and Ground Truth for Correct GS Samples on the PNG Dataset test split.

Caption	Image	GT	Ours
<p>In this picture there is a girl standing holding umbrella in her hand. She is wearing a hoodies and boots. Behind her there are trees, plants and sky.</p>			
<p>In the picture we can see a bench and on it we can see a paper with some text on it and beside it, we can see a person's leg on the bench and behind it we can see the wall.</p>			

Figure 7: Visualization of Images and Ground Truth for Failed GS Samples on the PNG Dataset test split.